Impact of Cell Density and Collagen Concentration on the Electromagnetic Properties of Dermal Equivalents in the Terahertz Band

Rui Zhang, *Student Member, IEEE,* Ke Yang, *Member, IEEE,* Qammer H. Abbasi, *Senior Member, IEEE,* Najah Abed AbuAli, and Akram Alomainy, *Senior Member, IEEE,*

***Abstract*—In this paper, the measurement of collagen gels and dermal equivalents (DEs) with three kinds of fibroblast cell densities and collagen concentrations is performed, respectively, using Terahertz-Time Domain Spectroscopy (THz-TDS) in transmission mode. With the objective to reduce the thickness uncertainty, an algorithm to extract material parameters and sample thickness of thin samples simultaneously is employed. The statistical mean and standard deviation of the refractive indexes and absorption coefficients in a THz band from 0.2 THz to 1.5 THz are presented. It is shown that the refractive indexes of DEs drop by around 10%, while the absorption coefficients decrease by 20% when cell density increases by one order from 0.1 M/ml to $1M/ml$. In addition, the complex refractive indexes of DEs with 3 mg/ml collagen are higher than those with 2 mg/ml, while the THz optical parameters of DEs with 2.5 mg/ml are the lowest. The obtained results indicate that the difference in the intrinsic biological features, initial cell density and collagen concentration changes the tissue hydration, which in turn brings changes to the electromagnetic properties.**

***Keywords*—Terahertz-Time Domain Spectroscopy, dermal equivalent, thickness extraction, material parameters**

I. Introduction

Nanotechnology with the aim of creating nano-devices with new functionalities can satisfy the need to reduce the size of the devices in Wireless Body Area Networks (WBANs) and motivate promising medical applications. Besides, the latest development in novel materials, like Graphene and its derivatives, namely, Graphene Nano-ribbons (GNRs) and Carbon Nano-tubes (CNTs), encourages the electromagnetic (EM) communication among nano-devices in the terahertz (THz) band (0.1-10 THz) inside the human body. Motivated by the increasing demand and technological advances in bio-medical field, the in-vivo nanonetworks represents a new and fascinating direction of research. Meanwhile, human activities would play an important roles in the channel modelling of the future THz communication and mm-wave communication, especially for the in-door communication [1]–[5]. However, there is a lack of studies on the channel medium, especially the existence of human body. It is because of the scarcity of the researches on the basic human tissues at the band of interest.

When THz wave propagates through lossy biological tissues, the channel exhibits peculiar characteristics which are different from those of more familiar wireless cellular and Wifi environments. Therefore, understanding the performance of THz wave inside tissue/cell is essential and important for channel modelling of in-vivo EM communication in the THz band [6]–[10]. Among all the researches, the characterisation of EM properties of human tissues in the THz band is the initial step for the study on the THz communication.

It is experimentally found that THz wave is strongly absorbed by liquid water [11], [12]. Such intensive absorption is due to the stretching and bending vibrational modes of the inter-molecular hydrogen bonds between the water molecules, falling into the THz region [13]. On one hand, high absorption restrains the THz communication in biological tissues with high water content. On the other hand, the THz wave is highly sensitive to water concentration, which means that slight changes in water proportion can be detected.

In the last decade, THz technology has been utilised as an effective analysis method to characterise the molecular dynamics of the bio-materials. Spectrally-resolved optical parameters, especially refractive index and absorption coefficient have been extensively studied to characterise different tissues at the THz band, such as blood, breast, liver, *etc.* in [14]–[16]. Among them, skin is a promising candidate because it is the most abundant human tissue and offers dynamic analysis due to its various hydration levels throughout the human body. Its material properties characertisation is an important advancement in the field to understand different phenomena. In past, several studies have been performed to characterise the THz electromagnetic properties of human skin in [17]–[20]. However, the presented parameters differ from each other, which could be caused by the difference in the type, state, specific layer and complexity of the human skin samples, *etc.* Such diversity in the parameters motivates us to study the intrinsic biological features and their influence on the material properties. It is extensively observed and demonstrated in THz imaging and spectroscopy that the tissue water content is the dominant contrast mechanism. How does the biological structure and features affect the water concentration in tissues and then change the material properties has not been studied. In order to address this problem, artificial skin samples allowing repeatable measurement are constructed and tested to investigate and reveal the intrinsic relations.

Rui Zhang, Ke Yang and Akram Alomainy are with Electronic Engineering and Computer Science, Queen Mary University of London, London (rui.zhang, k.yang, a.alomainy)@qmul.ac.uk

Qammer H. Abbasi is with School of Engineering, University of Glasgow, Glasgow qammer.abbasi@glasgow.ac.uk

Najah Abed AbuAli is with College of Information Technology, United Arab Emirates University, Al-Ain, UAE najah@uaeu.ac.ae

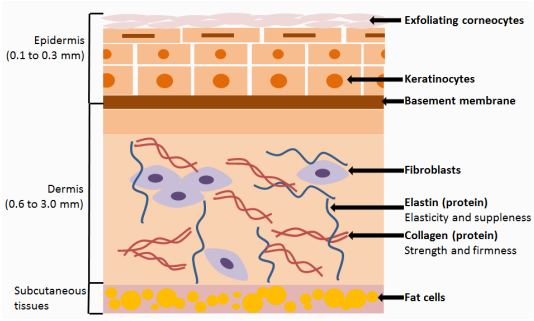

Figure 1. Schematic of human skin structure and constituent cell types. Skin is stratified composed of the epidermis, dermis and subcutaneous fat.The dermis is a layer rich in connective tissue and is divided into the papillary and reticular regions. The dermis contains many cell types including fibroblasts that make collagen and other ECM molecules that provide skin mechanical toughness.

Skin can be divided into three main layers: epidermis, dermis and subcutaneous fat as shown in Fig. 1. Among them, dermis is the thickest layer comprised of extracellular matrix (ECM), fibroblasts, vascular endothelial cells and skin appendages. Collagen is the main structural protein of the ECM in various connective tissues in animal bodies. Type I collagen is the most abundant collagen in the human body, which forms large, eosinophilic fibers known as collagen fibers. Dermal equivalent (DE) is developed by seeding dermal fibroblast cells in collagen gel to progressively re-organise the lattice [21]. As a substitute for normal skin in vivo, DEs have been used in various fields of skin biology, pharmacotoxicology and also as a replacement for human skin in clinical applications [22], [23].

It has been shown that dermal equivalent contracts more at high fibroblast concentration and low collagen concentration [21]. The contraction is the phenomenon that the lattice is contracted and water is squeezed out when fibroblast cells are incorporated into hydrated collagen lattices [21]. Inspired by this observation, we investigated the effect of the fibroblast cell density and collagen concentration on the THz electromagnetic properties of artificial skin by making collagen gels and DEs, and testing various samples using THz-TDS.

A preliminary study of collagen with different cell numbers has been presented in [24]. However, the effect of collagen concentration was not considered in the literature. Furthermore, a limited number of samples and measurements bring many uncertainties to the results. The traditional sandwich technique using two plates to press the sample could cause unnecessary force to the sample, which could negatively affect its biological features [25]. The sample thickness is not accurately determined in the experiment nor signal processing, which generates great uncertainties to the material parameters extraction.

In our work, we profoundly investigated the impact of fibroblast cell density and collagen concentration on the material properties of artificial skin samples in the THz band with more confidence by developing various samples, conducting repeated measurements and utilising advanced extraction algorithms.

The main contributions of this paper are summarised as follows. First, artificial DEs were constructed as alternatives to excised human skin, and collagen gels without seeding cells were made as a control study to completely reveal the impacts. In addition, statistical description of the material parameters has been obtained by conducting three repeated experiment on five samples for each scenario with THz-TDS system operating in transmission mode. Moreover, due to the softness of the sample, slight press in measuring thickness with caliper or strength from the sample holder can bring errors to the thickness value. Thus, two techniques were utilised to alleviate the errors introduced by the thickness uncertainty. On one hand, the samples were carefully mounted on one TPX (poly-4-methyl pentene-1) plate without squeezing in the operation; on the other hand, an algorithm that can extract optical parameters and thickness simultaneously [26] was implemented in data processing. Finally, the conclusions drawn from the statistical results of material parameters provide strong fundamentals for the THz channel characterisation of the in-vivo nanonetworks.

The rest of this paper is organised as follow. In Section II, the materials, cell cultivation and procedures to construct artificial collagen gels and DEs are provided. Section III introduces the THz-TDS system, sample mounting in the operation and the extraction algorithm to obtain optical parameters and sample thickness simultaneously. In Section IV, the statistical mean and standard deviation of refractive indexes and absorption coefficients of various samples are presented. The effect of collagen concentration and cell density on the material parameters of artificial skin are analysed and discussed. Finally, conclusions are drawn in Section V.

II. Artificial Skin Samples Cultivation

A. Cell Culture Medium

The medium used for serial cultivation of fibroblast cells consists of Dulbecco's Modified Eagle Medium (DMEM) supplemented with 10 % Fetal Bovine Serum (FBS), 2 mM L-glutamine. Antibiotics can also be added at final concentrations of 50 units/ml penicillin and 50 g/ml streptomycin. This growth medium supplies the cells with the essential nutrients such as carbohydrates, vitamins, glucose, minerals, $etc.$

B. Fibroblasts Cultivation

Frozen 3T3 cells are thawed into a T75 flask containing 15 ml DMEM medium and incubated at 37 $^{\circ}C$ in a 5% CO_2 atmosphere to allow attach. Cells are routinely passaged by trypsinisation with 0.05% trypsin-EDTA. All cell cultivation is performed in a laminar flow hood under aseptic conditions in accordance with standard tissue culture technique.

C. Dermal Equivalents

Collagen lattices are prepared according to the protocol provided by life technologies [27]. The solution is made up in the following parts: collagen (type I rat tail) makes up 8 parts of final mix, 10X Minimum Essential Medium (MEM) makes 1 part and Fetal Bovine Serum (FBS) containing the desired number of fibroblast cells makes 1 part. NaOH is dropwise added to adjust pH to around 7.2 until the mix

became orange/pink colour. The collagen gels are incubated for gelation at 37 $^{\circ}C$, 5% CO_2 for approximately 15 minutes.

Dermal equivalents are constructed by casting fibroblasts with different densities into rat tail collagen solution and allowing the solution to solidify and contract. When fibroblast cells are incorporated into hydrated collagen lattices, the lattice is contracted and water is squeezed out in the contraction process.

With regards to the selection of cell and collagen levels, a literature survey of the conditions for the preparation of DEs reveals that the initial collagen concentration in the dermal mixture varied from 0.9 mg/ml to 2.9 mg/ml [28], [29]. The initial fibroblast concentration varied from $1*10^5$ cells/ml [28] to $1*10^6$ cells/ml [30]. Thus in our study, in accordance with the reported conditions, three cell densities $0.1M/ml$, 0.5 M/ml and 1 M/ml are selected and the collagen concentration are chosen as 2 mg/ml, 2.5 mg/ml and 3 mg/ml. All of these dermal mixtures were prepared in duplicate to model the effect of these variables on the THz electromagnetic parameters of artificial skin.

Due to the fact that biological tissues with high water content are highly absorptive to the THz wave, artificial skin samples in our experiment are required to be thin enough to enable the THz signal transmit through the sample and come to the detector with proper intensity. Meanwhile, it is experimentally demonstrated that the initial gel thickness had no appreciable effect on the contraction of the DE [29]. Therefore, we made the initial sample thickness at about 100 μm by controlling the volume of the collagen solution in 12-well plastic culture dishes. This thickness was experimentally validated to maintain a reasonable transmitted signal at the beginning of our measurement.

III. Experimental Methodology and Techniques

Three independent experiments were conducted for each sample, and five duplicate samples were tested. Statistical information including the mean values and deviation of the material parameters were obtained in our investigation.

A. Terahertz-Time Domain Spectroscopy Setup

THz-TDS is a spectroscopic technique that uses ultrashort pulses of THz radiation to probe materials. The TDS in transmission mode used in our experiment is shown in Fig. 2. The delay stage is mechanically controlled. It changes the relative path length of the probe beam to the pump beam to facilitate the mapping of a whole THz pulse. Using multiple path lengths is equivalent to measuring the THz electric field at multiple instants in time. The time domain waveform of the THz signal is obtained by connecting the multiple measurements in a time line of the optical delays. The spectrum of the THz pulses is obtained by using Fast Fourier Transform (FFT). More details about this setup can be found in [31].

B. Sample Mounting

Instead of sandwiching samples, the sample was mounted on one TPX plate as shown in Fig. 3(b). TPX is used as a mounting plate due to its unique properties in the THz

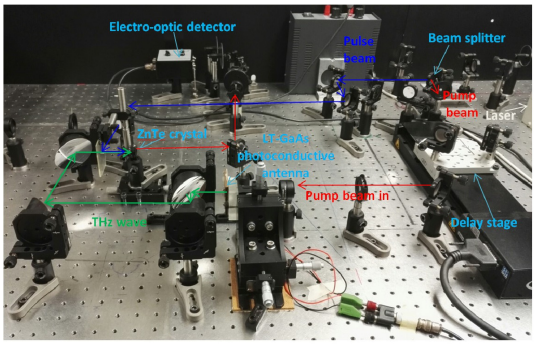

Figure 2. THz-TDS in transmission mode at Queen Mary University of London

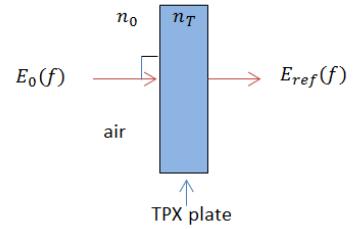

(a) Reference measurement

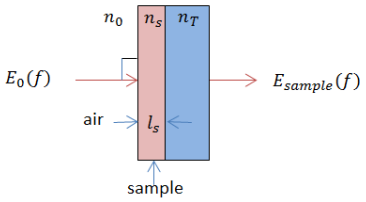

(b) Sample measurement

Figure 3. Geometry for sample measurement used in this study

spectral domain. Its absorption coefficient is very low which is less than 1 cm^{-1} and refractive index is 1.46, and both are non-dispersive in 0.1 to 4 THz [32]. In the measurement orientation, the incident THz signal encounters the sample first and then the TPX before collected from the receiver. Therefore, the reference signal is the transmission through a blank TPX alone as shown in Fig. 3(a).

C. Data Processing

The following assumptions are made to derive the analytical transfer function,

- The investigated samples are homogeneous.
- The roughness and curvature of the irradiated materials, as well as scattering effects at the surfaces and inside the materials are neglected. All surfaces are assumed to be perfectly flat and parallel.
- The THz wave impinges on the samples orthogonally, thus the electromagnetic response of the media is linear.

A THz signal transmitted through a sample is influenced by the absorption and dispersion of the sample. A change in the transmitted signal hence relates to the optical properties of the sample, which can be extracted via the physical

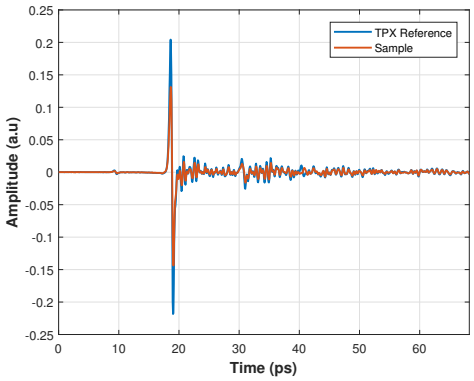

(a) Time domain

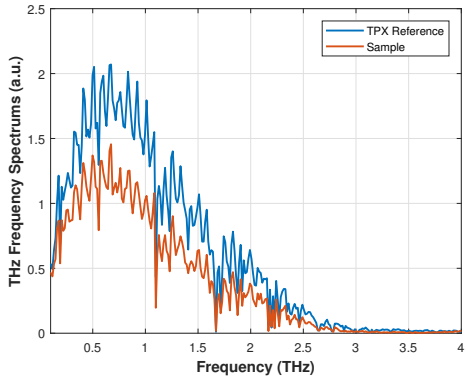

(b) Sample measurement

Figure 4. THz waveforms in (a) time domain and (b) frequency domain for DE with 2 mg/ml collagen and 0.1 M/ml fibroblast cells.

models of a propagating wave. The measured signal is in fact a convolution between the incident THz field, the optical probe pulse, and the system response. The original measurement data from THz-TDS system are the received electric field in time domain. Optical parameters extraction requires the amplitude and phase information of signal, thus FFT is evaluated of the time-domain measurements of sample and reference, E_{sample} and E_{ref}, respectively. The original time information for one test of TPX plate reference and DE sample with 2 mg/ml collagen and 0.1 M/ml fibroblasts in our experiment is plotted as Fig. 4(a), and the frequency amplitude after conducting FFT is shown in Fig. 4(b).

Normalising the sample spectrum by the reference, as $E_{sample}(f)/E_{ref}(f)$, results in the complex transfer function of the sample in the frequency domain. Hence, the transfer function becomes [33],

$$H(f) = \hat{\tau}(f)e^{-j(n_s(f)-n_0)\frac{2\pi fd}{c}}e^{-\kappa_s(f)\frac{2\pi fd}{c}}FP(f) \quad (1)$$

$$FP(f) = \frac{1}{1-(\frac{\hat{n}_s(f)-n_0}{\hat{n}_s(f)+n_0}\frac{\hat{n}_s(f)-n_T}{\hat{n}_s(f)+n_T})e^{-4j\hat{n}_s(f)\pi fd/c}} \quad (2)$$

where c is the speed of light in vacuum, d is the transmission distance, n_0 is the refractive index of air, n_T is the refractive index of the TPX material and $\hat{n}_s(f)$ is the complex refractive index of the tested material. $\hat{n}_s(f) = n_s(f) - i\kappa_s(f)$, where $n_s(f)$ is the refractive index and $\kappa_s(f)$ is the extinction coefficient. $FP(f)$ presents the Fabry-Perot effect due to the multiple reflections inside the sample.

The propagation of signal through both the sample and reference is calculated using well-established impedance and reflection interactions for multiple layers. The transmission coefficient is given by,

$$\hat{\tau}(f) = \frac{2\hat{n}_s(f)(n_0+n_T)}{(\hat{n}_s(f)+n_T)(\hat{n}_s(f)+n_0)} \quad (3)$$

In the case of thin film materials, the THz pulse transmission is greatly affected by multiple reflections. In order to dis-entangle the FP effect and measure the material parameters with high accuracy, an iterative fitting process based on a polynomial fit of the transmission parameters is employed in this paper. It enables a confident extraction of the refractive index and absorption coefficient.

Sample thickness is one of the various sources of uncertainty appearing in measurement and throughout the parameter extraction process which can strongly negatively affect the results [34], [35]. Therefore, correct determination of the sample thickness is critical for accurate optical parameters extraction. However, it is difficult to measure the accurate thickness of the thin and supple sample film. A slight strength from caliper could change the value, resulting that the thickness of the sample is not generally known with a sufficient accuracy. To solve this problem, an iterative process of calculation is highly demanded. Therefore, in this paper a robust algorithm to obtain both the thickness and the complex refractive index of the sample simultaneously is utilised [26].

By measuring the sample thickness with an electronic caliper, we obtain an initial value for the variable d. As a first step the raw estimations of n_s and α_s can be obtained with the initial thickness value d by neglecting the FP effect in Eq. 2 with the following expressions,

$$n_s(f) = n_0 - \frac{c}{2\pi fd}(\phi_{samp}(f) - \phi_{ref}(f)) \quad (4)$$

where $\phi_{samp}(f)$ and $\phi_{ref}(f)$ are the phases of the measured transmission coefficient over the reference material and sample, respectively.

$$\kappa_s(f) = -\frac{c}{2\pi fd}ln(|H(f)|\frac{2\hat{n}_s(f)(n_0+n_T)}{(\hat{n}_s(f)+n_T)(\hat{n}_s(f)+n_0)} \quad (5)$$

$$\alpha_s(f) = \frac{4\pi f}{c}\kappa_s(f) \quad (6)$$

where $\alpha_s(f)$ is the absorption coefficient of sample at frequency f.

However, the extracted coefficient in Eq. 4 and Eq. 6 are affected by fake oscillations due to the neglected FP effect. A polynomial fit of the material parameters, variable order and fitting range is implemented to catch the real physical frequency behaviour and remove the FP oscillations.

Afterwards, the full theoretical transfer function $H(f)$ including the FP in Eq. 1 is calculated. Then we compare the results with the experimental transfer function to infer new best values for n_s, α_s and d. Therefore, the second step

is to minimise the following error function with a numerical optimisation on the n_s and α_s for different fixed values of d [26],

$$\triangle H = \sum_f |H_{the}(f) - H_{exp}(f)| \tag{7}$$

where $H_{the}(f)$ is the theoretical value in in Eq. 1 and $H_{exp}(f)$ is the experimental value.

The Nelder-mead simplex algorithm [36] is utilised to perform a numerical optimisation. Two scalar parameters ζ, ψ are used to define the new values of real refractive index and extinction coefficient as [26],

$$n_{new}(f) = \zeta(n_{old}(f) - 1) + 1 \tag{8}$$

$$k_{new}(f) = \psi k_{old}(f) \tag{9}$$

The reason for this definition is that the induced shift by the sample does not scale with n but is related to $(n-1)$. Thus, the order of the magnitude of the two parameters is comparable, which is favorable for numerical optimisation.

For each value of d, new values of $n(f,d)$ and $\alpha(f,d)$ are calculated by Eq. 4 and Eq. 6, filtered with the polynomial fit, and then optimised minimising $\triangle H$. Subsequently, we plot $\triangle H$ at varying values of d to find the minimum of $\triangle H$ at d_{min} value, which corresponds to the sample thickness. For example, the error as a function of the sample thickness in one test in our experiment is illustrated in Fig. 5. The thickness corresponding to the minimum error is the optimal instantaneous thickness for the tested sample.

The fitting process is then repeated, starting from $n(f,d_{min})$, $\alpha(f,d_{min})$, and d_{min}. It is worthwhile noting that the parametrisations of n and α through the scalar ζ and ψ does not change their frequency behaviours, which are still those inferred from the first step and can be affected by the filtering process. Thus, the final step is performing an optimisation of the optical parameters at every frequency step f_i using the error function [37],

$$\triangle H(f_i) = |H_{the}(f_i) - H_{exp}(f_i)| \tag{10}$$

The starting values for n and α are the optimal ones obtained in the previous step. The parametrisation is the same as Eq. 8 and Eq. 9 using the same algorithm, while d is always kept fixed to the optimal value estimated before. This last optimisation reshapes the frequency features of the material parameters that may have been distorted or erased by the first step evaluation and filtering process. This new set of curves of n and α can be used for a new optimisation cycle starting again from the step one. Especially for samples with short optical paths, the optimisation must be repeated several times to find reliable values of the sample thickness and the optical parameters.

IV. Analysis and Parametric Studies

The refractive indexes and absorption coefficients of collagen gels with three different collagen concentrations, and DEs with three different collagen concentrations and three different cell densities are shown in Figs. 6, 7, 8. The results show that, in general, the refractive indexes decrease with frequency in the band between 0.2 THz and 1.5 THz, while the absorption coefficients increase with frequency

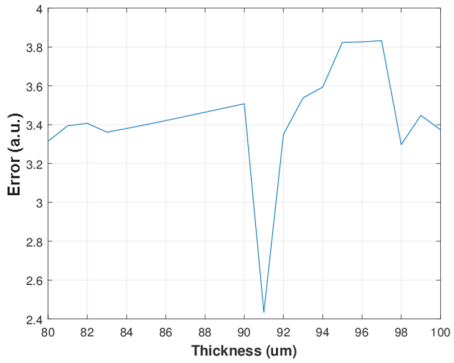

Figure 5. Error between the theoretical model and measured signals according to Eq. 7. The intermediate stepping distance is $1\mu m$

regardless of collagen and cell levels. The fluctuations and peaks can be caused by the molecules of water vapour. As the absorption coefficients of water vapour has multiple resonant peaks within the THz band and the water vapour is not excluded in our experiment.

A. Effect of Cell Density

a) Without cells: The collagen gels without cells are considered as a control set to study the effect of the cell density on the EM material parameters. The parameters of collagen gels are the highest comparing with DEs with cells for all three different collagen concentrations. Take samples with 2 mg/ml collagen as an example, the refractive indexes of collagen gels goes down from 2 to 1.5 in the frequency band of interest, while the absorption coefficients increase from around 130 cm^{-1} to 200 cm^{-1}.

b) With cells: When it comes to DEs, both refractive indexes and absorption coefficients decrease with the fibroblasts density in the DEs. Take 2 mg/ml as an example as well, the indexes of DEs with 0.1 M/ml cells reduces from 1.8 to 1.5, while DEs with 0.5 M/ml and 1 M/ml cells goes down from 1.8 to 1.2 and 1.6 to 1.2, respectively. Furthermore, the absorption coefficients of DEs with 0.1 M/ml cell density experience a rise from about 91 cm^{-1} to 150 cm^{-1}, while the other two types go up from about 80 cm^{-1} to 130 cm^{-1} and 76 cm^{-1} to 105 cm^{-1}, respectively. In terms of the samples with collagen concentrations 2.5 mg/ml and 3 mg/ml, both refractive indexes and absorption coefficients decrease with the cell density as shown in Fig. 7 and Fig. 8, respectively.

The primary reason is that water is squeezed out from DEs in the contraction process and the squeezed water volume increases with the initial cell density. It means that when keeping other factors the same and fibroblast density be the only variation, the water content in DE samples decreases with the cell density. Thus the THz electromagnetic parameters drop with cell density. The obtained results are in line with the gel contraction phenomenon and high sensitivity of THz signal to water content.

B. Effect of Collagen Concentration

The comparative results of refractive indexes and absorption coefficients of samples with three different collagen

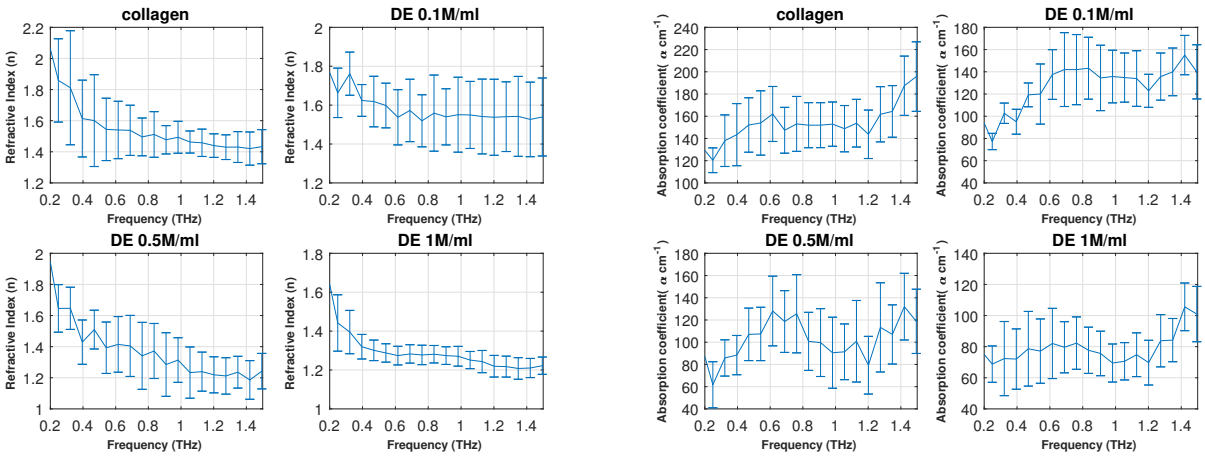

(a) Refractive index (b) Absorption coefficient

Figure 6. THz complex optical parameters of collagen gels and DEs with different fibroblasts densities, and the collagen concentration is 2 mg/ml. The line and error bar represent the mean value and standard deviation of the optical parameters.

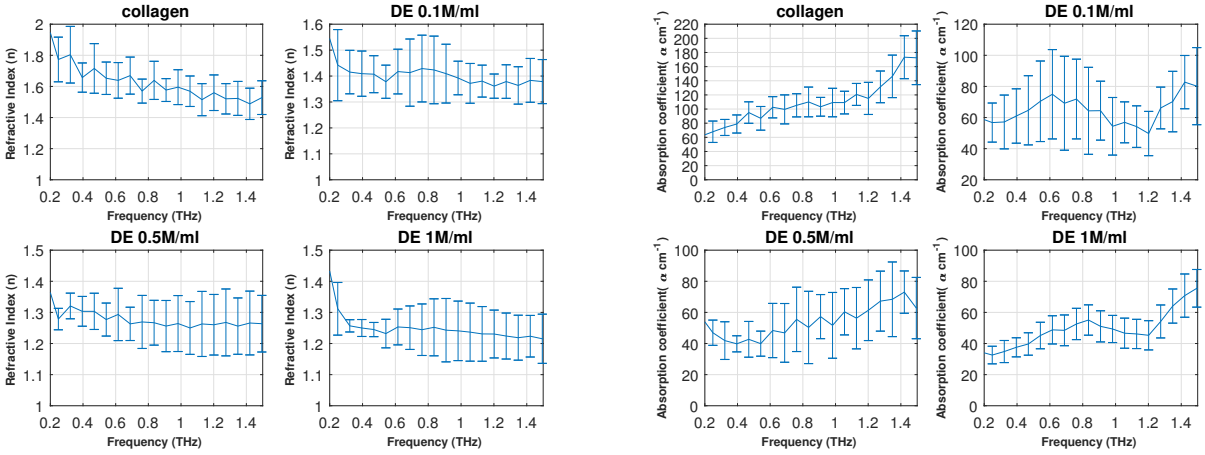

(a) Refractive index (b) Absorption coefficient

Figure 7. THz complex optical parameters of collagen gels and DEs with different fibroblasts densities, and the collagen concentration is 2.5 mg/ml.

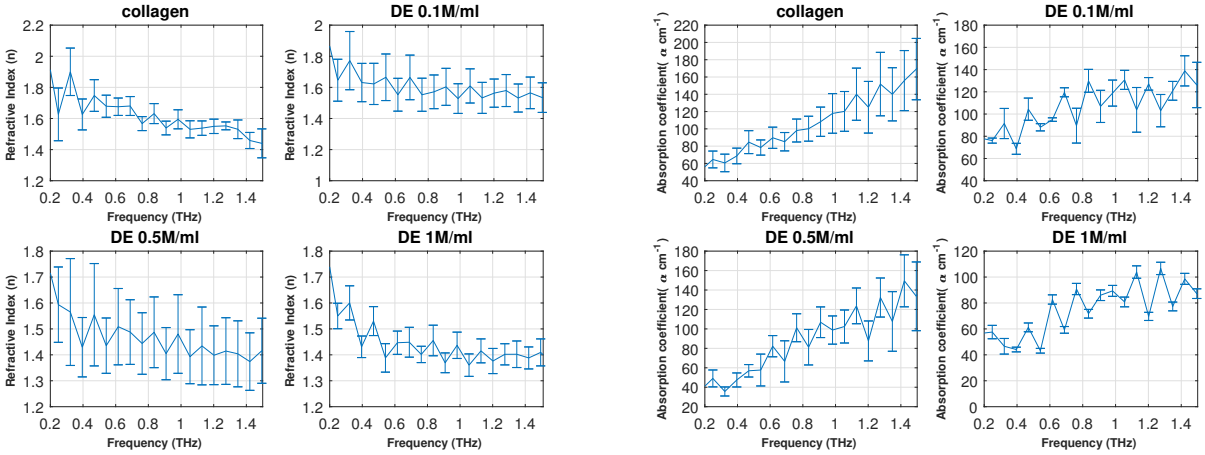

(a) Refractive index (b) Absorption coefficient

Figure 8. THz complex optical parameters of collagen gels and DEs with different fibroblasts densities, and the collagen concentration is 3 mg/ml.

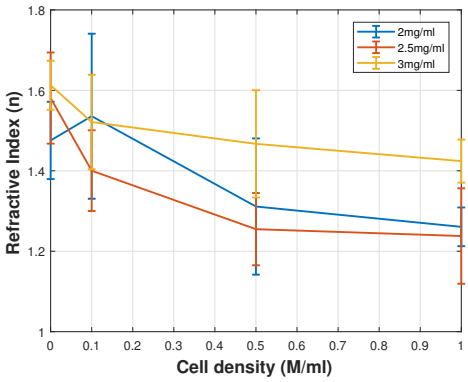

(a) Refractive index

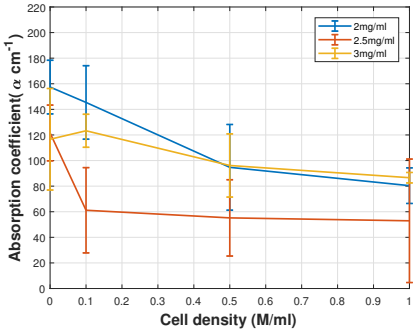

(b) Absorption coefficient

Figure 9. Complex optical parameters at 1 THz vs cell density with different collagen concentrations.

concentrations at the same cell density can be seen vertically from Figs. 6, 7, 8.

With regards to the collagen gels without cells, generally, the refractive indexes and absorption coefficients of gels with low collagen concentration are high. The main reason is that low initial collagen concentration means high tissue hydration. In terms of the DEs with fibroblast cells seeded, the contraction phenomenon bring some changes. In general, at the same cell density, the parameters of samples with 3 mg/ml collagen are the highest, while the values of DEs with 2.5 mg/ml collagen are the smallest among three concentrations.

In order to clearly show the quantitative relationship between optical parameters and the collagen concentration and cell densities, the extracted refractive indexes and absorption coefficients of various scenarios at 1 THz are shown in Fig. 9. In summary, the refractive indexes drop approximately 10%, while the absorption coefficients decrease about 20% when cell density in DEs increases by one order from 0.1 M/ml to $1M/ml$. Generally, both refractive indexes and absorption coefficients of DEs with 3 mg/ml are the highest while the ones of 2.5 mg/ml have the least values.

It is primarily because that higher initial collagen concentration means less water content in the DEs. However, as demonstrated that DE contracts more at a low concentration. Thus, the least water is squeezed out in the contraction process of DEs with 3 mg/ml compared with 2 mg/ml and 2.5 mg/ml. Even though the initial water content of DEs with 3 mg/ml is the least, after the contraction process, the water content of them can be the most ones. In terms of the DEs with 2.5 mg/ml collagen, two contrary variation trends of hydration make the samples contain the least water after contraction. Therefore, they have the smallest optical parameters comparatively. The relative water content of DEs with different collagen concentrations is not determined, which causes the refractive indexes and absorption coefficients of DEs in different collagen concentrations can intersect as shown in Fig. 9.

The standard deviation of the obtained results is generated by some inevitable uncertainties in the sample preparation and THz test. For example, we count cells with haemocytometer when seed cells inside the collagen mixture, but it is challenging to make sure the cell numbers are totally the same for each gel. Slight difference in cell numbers may affect the gel contraction process and then affect the water content in DEs. Besides, the gels might be slightly stretched when taking out from the well plate in different extents, which is the main factor causing the thickness of each gel different. In our repetitive experiments, some of the samples with the same cell and collagen levels were prepared at the same time, while others were constructed in different days. Thus, the tests did in different days might be negatively affected in different extents by the water vapour.

V. Conclusions

The material parameters of artificially synthesised collagen gels and dermal equivalents in the frequency band 0.2 THz to 1.5 THz are measured and presented. The effect of the fibroblast cell density and collagen concentration on the optical properties has been comparatively studied and analysed. Generally, the refractive indexes of DEs in the frequency band of interest drop approximately 10%, while the absorption coefficients decrease about 20% when cell density increases by one order from 0.1 M/ml to $1M/ml$. Besides, the refractive indexes and absorption coefficients of DEs with 3 mg/ml collagen are the highest, while the values of DEs with 2.5 mg/ml are the lowest.

It is concluded that the material parameters at the THz band is mainly dependent on the water concentration. Furthermore, the intrinsic biological structure and features such as cell density and collagen concentration change the tissue hydration, and in turn brings changes to the material properties. Specifically, more water is squeezed out in the contraction at high fibroblast concentration and low collagen concentration. Therefore, the refractive indexes and absorption coefficients of DEs are low at high cell density and low collagen levels. The obtained results help understand the interaction of the THz wave with biological tissues and the diversity of material parameters of real human skin. This, in turn, paves the road for efficient and comprehensive electromagnetic communication channel modelling and system performance predictions for future nano-scale in-vivo networks.

VI. Acknowledgement

Many thanks to the CSC (China Scholarship Council) for supporting the first author's research studies at Queen Mary University of London (QMUL), UK.

REFERENCES

[1] S. Geng, J. Kivinen, X. Zhao, and P. Vainikainen, "Millimeter-wave propagation channel characterization for short-range wireless communications," *IEEE Transactions on Vehicular Technology*, vol. 58, no. 1, pp. 3–13, 2009.

[2] M. R. Akdeniz, Y. Liu, M. K. Samimi, S. Sun, S. Rangan, T. S. Rappaport, and E. Erkip, "Millimeter wave channel modeling and cellular capacity evaluation," *IEEE journal on selected areas in communications*, vol. 32, no. 6, pp. 1164–1179, 2014.

[3] T. S. Rappaport, G. R. MacCartney, M. K. Samimi, and S. Sun, "Wideband millimeter-wave propagation measurements and channel models for future wireless communication system design," *IEEE Transactions on Communications*, vol. 63, no. 9, pp. 3029–3056, 2015.

[4] C. Han, A. O. Bicen, and I. F. Akyildiz, "Multi-ray channel modeling and wideband characterization for wireless communications in the terahertz band," *IEEE Transactions on Wireless Communications*, vol. 14, no. 5, pp. 2402–2412, 2015.

[5] J. M. Jornet and I. F. Akyildiz, "Channel modeling and capacity analysis for electromagnetic wireless nanonetworks in the terahertz band," *IEEE Transactions on Wireless Communications*, vol. 10, no. 10, pp. 3211–3221, 2011.

[6] Q. H. Abbasi, H. El Sallabi, N. Chopra, K. Yang, K. A. Qaraqe, and A. Alomainy, "Terahertz channel characterization inside the human skin for nano-scale body-centric networks," *IEEE Transactions on Terahertz Science and Technology*, vol. 6, no. 3, pp. 427–434, 2016.

[7] R. Zhang, K. Yang, Q. H. Abbasi, K. A. Qaraqe, and A. Alomainy, "Analytical modelling of the effect of noise on the terahertz in-vivo communication channel for body-centric nano-networks," *Nano Communication Networks*, 2017.

[8] R. Zhang, K. Yang, Q. Abbasi, K. Qaraqe, and A. Alomainy, "Analytical characterisation of the terahertz in-vivo nano-network in the presence of interference based on ts-ook communication scheme," *IEEE Access*, vol. 5, pp. 10172–10181, 2017.

[9] Q. H. Abbasi, M. U. Rehman, K. Qaraqe, and A. Alomainy, *Advances in body-centric wireless communication: Applications and state-of-the-art*. Institution of Engineering and Technology, 2016.

[10] Q. H. Abbasi, A. A. Nasir, K. Yang, K. Qaraqe, and A. Alomainy, "Cooperative in-vivo nano-network communication at terahertz frequencies," *IEEE Access*, 2017.

[11] J. Kindt and C. Schmuttenmaer, "Far-infrared dielectric properties of polar liquids probed by femtosecond terahertz pulse spectroscopy," *The Journal of Physical Chemistry*, vol. 100, no. 24, pp. 10373–10379, 1996.

[12] K. Jeong, Y.-M. Huh, S.-H. Kim, Y. Park, J.-H. Son, S. J. Oh, and J.-S. Suh, "Characterization of blood using terahertz waves," *Journal of biomedical optics*, vol. 18, no. 10, pp. 107008–107008, 2013.

[13] E. Pickwell and V. Wallace, "Biomedical applications of terahertz technology," *Journal of Physics D: Applied Physics*, vol. 39, no. 17, p. R301, 2006.

[14] C. B. Reid, G. Reese, A. P. Gibson, and V. P. Wallace, "Terahertz time-domain spectroscopy of human blood," *IEEE Transactions on Terahertz Science and Technology*, vol. 3, no. 4, pp. 363–367, 2013.

[15] G. Png, J. Choi, B. W. Ng, S. Mickan, D. Abbott, and X. Zhang, "The impact of hydration changes in fresh bio-tissue on thz spectroscopic measurements," *Physics in Medicine and Biology*, vol. 53, no. 13, p. 3501, 2008.

[16] T. Bowman, M. El-Shenawee, and S. G. Sharma, "Terahertz spectroscopy for the characterization of excised human breast tissue," in *Microwave Symposium (IMS), 2014 IEEE MTT-S International*, pp. 1–4, IEEE, 2014.

[17] A. Fitzgerald, E. Berry, N. Zinov'ev, S. Homer-Vanniasinkam, R. Miles, J. Chamberlain, and M. Smith, "Catalogue of human tissue optical properties at terahertz frequencies," *Journal of Biological Physics*, vol. 29, no. 2-3, pp. 123–128, 2003.

[18] E. Berry, A. J. Fitzgerald, N. N. Zinov'ev, G. C. Walker, S. Homer-Vanniasinkam, C. D. Sudworth, R. E. Miles, J. M. Chamberlain, and M. A. Smith, "Optical properties of tissue measured using terahertz-pulsed imaging," in *Medical Imaging 2003*, pp. 459–470, International Society for Optics and Photonics, 2003.

[19] E. Pickwell, B. Cole, A. Fitzgerald, M. Pepper, and V. Wallace, "In vivo study of human skin using pulsed terahertz radiation," *Physics in Medicine and Biology*, vol. 49, no. 9, p. 1595, 2004.

[20] E. Pickwell, A. J. Fitzgerald, B. E. Cole, P. F. Taday, R. J. Pye, T. Ha, M. Pepper, and V. P. Wallace, "Simulating the response of terahertz radiation to basal cell carcinoma using ex vivo spectroscopy measurements," *Journal of Biomedical Optics*, vol. 10, no. 6, pp. 064021–064021, 2005.

[21] E. Bell, B. Ivarsson, and C. Merrill, "Production of a tissue-like structure by contraction of collagen lattices by human fibroblasts of different proliferative potential in vitro," *Proceedings of the National Academy of Sciences*, vol. 76, no. 3, pp. 1274–1278, 1979.

[22] M. Regnier, D. Asselineau, and M. Lenoir, "Human epidermis reconstructed on dermal substrates in vitro: an alternative to animals in skin pharmacology," *Skin Pharmacology and Physiology*, vol. 3, no. 2, pp. 70–85, 1990.

[23] M. Ponec, "Reconstruction of human epidermis on de-epidermized dermis: expression of differentiation-specific protein markers and lipid composition," *Toxicology in vitro*, vol. 5, no. 5-6, pp. 597–606, 1991.

[24] N. Chopra, K. Yang, J. Upton, Q. H. Abbasi, K. Qaraqe, M. Philpott, and A. Alomainy, "Fibroblasts cell number density based human skin characterization at thz for in-body nanonetworks," *Nano Communication Networks*, vol. 10, pp. 60–67, 2016.

[25] F. Grinnell, "Fibroblast biology in three-dimensional collagen matrices," *Trends in cell biology*, vol. 13, no. 5, pp. 264–269, 2003.

[26] A. Taschin, P. Bartolini, J. Tasseva, and R. Torre, "Thz time-domain spectroscopic investigations of thin films," *Measurement*, 2017.

[27] Available at https://assets.thermofisher.com/TFS-Assets/LSG/manuals/A1064401_Bovine_collagen_I_PI.pdf, Life technologies.

[28] F. Grinnell, A. Takashima, and C. Lamke-Seymour, "morphological appearance of epidermal cells cultured on fibroblast-reorganized collagen gels," *Cell and tissue research*, vol. 246, no. 1, pp. 13–21, 1986.

[29] P. Rompré, F. A. Auger, L. Germain, V. Bouvard, C. L. Valle, J. Thibault, and A. Le Duy, "Influence of initial collagen and cellular concentrations on the final surface area of dermal and skin equivalents: a box-behnken analysis," *In vitro cellular & developmental biology*, vol. 26, no. 10, pp. 983–990, 1990.

[30] F. Grinnell and C. R. Lamke, "Reorganization of hydrated collagen lattices by human skin fibroblasts," *Journal of cell science*, vol. 66, no. 1, pp. 51–63, 1984.

[31] O. Sushko, *Terahertz dielectric study of bio-molecules using time-domain spectrometry and molecular dynamics simulations*. PhD thesis, Queen Mary University of London, 2014.

[32] J. Birch and E. Nicol, "The fir optical constants of the polymer tpx," *Infrared physics*, vol. 24, no. 6, pp. 573–575, 1984.

[33] L. Duvillaret, F. Garet, and J.-L. Coutaz, "A reliable method for extraction of material parameters in terahertz time-domain spectroscopy," *IEEE Journal of selected topics in quantum electronics*, vol. 2, no. 3, pp. 739–746, 1996.

[34] L. Duvillaret, F. Garet, and J.-L. Coutaz, "Highly precise determination of optical constants and sample thickness in terahertz time-domain spectroscopy," *Applied optics*, vol. 38, no. 2, pp. 409–415, 1999.

[35] W. Withayachumnankul, B. M. Fischer, H. Lin, and D. Abbott, "Uncertainty in terahertz time-domain spectroscopy measurement," *JOSA B*, vol. 25, no. 6, pp. 1059–1072, 2008.

[36] J. C. Lagarias, J. A. Reeds, M. H. Wright, and P. E. Wright, "Convergence properties of the nelder–mead simplex method in low dimensions," *SIAM Journal on optimization*, vol. 9, no. 1, pp. 112–147, 1998.

[37] M. Scheller, "Real-time terahertz material characterization by numerical three-dimensional optimization," *Optics express*, vol. 19, no. 11, pp. 10647–10655, 2011.